

Climatic Variation Drives Loss and Restructuring of Carbon and Nitrogen in Boreal Forest Wildfire

Johan A. Eckdahl^{1,2}, Jeppe A. Kristensen³, and Daniel B. Metcalfe²

¹Department of Physical Geography and Ecosystem Science, Lund University, Lund, Sweden

²Department of Ecology and Environmental Science, Umeå University, Umeå, Sweden

³School of Geography and the Environment, University of Oxford, Oxford, United Kingdom

Correspondence: Johan Eckdahl (Johan.Eckdahl@nateko.lu.se)

Abstract. The boreal forest landscape covers approximately 10% of the earth's land area and accounts for almost 30% of the global annual terrestrial sink of carbon (C). Increased emissions due to climate change-amplified fire frequency, size and intensity threaten to remove elements such as C and nitrogen (N) from forest soil and vegetation at rates faster than they accumulate. This may result in large areas within the region becoming a net source of greenhouse gases creating a positive feedback loop with a changing climate. Meter-scale estimates of per area fire emissions are regionally limited and knowledge of their relation to climate and ecosystem properties is sparse. This study sampled 50 separate Swedish wildfires, which occurred during an extreme fire season in 2018, providing quantitative estimates of C and N loss due to fire along a climate gradient. Mean annual precipitation had strong positive effects on total fuel, which was the strongest driver for increasing C and N losses, while mean annual temperature (MAT) had greater influence on both pre- and postfire organic layer soil bulk density and C:N ratio which had mixed effects on C and N losses. Significant fire-induced loss of C was estimated in the 50 plots comparable to estimates in similar Eurasian forests but approximately a quarter of those found in typically more intense North American boreal wildfires. N loss was insignificant though a large amount of fire affected fuel was conserved in a low C:N surface layer of char in proportion to increased MAT. These results reveal the large discrepancies of C and N losses between global regions and variability across local climate conditions. A need exists to better incorporate these factors into models to improve estimates of global emissions of C and N due to fire in future climate scenarios. Additionally, this study demonstrated a linkage between climate and the extent of charring of residual soil fuel and discusses its potential for altering C and N dynamics in postfire recovery.

Copyright statement. TEXT

1 Introduction

Worldwide, boreal forests cover approximately 10% of land area (Keenan et al., 2015) and account for a net C sink into plants and soil of 0.31 ± 0.19 Pg of C per year, equivalent to $27.3 \pm 16.7\%$ of the planet's terrestrial C sink (Tagesson et al., 2020). This sink plays a pivotal role in the greenhouse gas content of the atmosphere (Lemprière et al., 2013). Low temperatures and

often waterlogged soil conditions slow decomposition of centuries of litter additions resulting in the build up of thick layers of soil organic material where the majority of C is stored (Malhi et al., 1999; Rapalee et al., 1998). The balance of C transferred between atmospheric and terrestrial stocks on the yearly timescale is dictated by rates of terrestrial net primary production and respiration which are themselves controlled by temperature, moisture and nitrogen (N) availability (Deluca and Boisvenue, 2012).

The predominant disturbance to this C balance in the boreal region are yearly outbreaks of wildfires which reoccur in individual forest stands at the centurial timescale (Bond-Lamberty et al., 2007). Among the immediate effects of fire are a substantial release of C to the atmosphere from soil and vegetation (Schultz et al., 2008) as well as physical restructuring of the habitat through varying degrees of over- and understory removal and changes in soil properties such as bulk density (Certini, 2005). Further, bioavailability of energy sources and nutrients is substantially affected as elements such as C and N are lost and their chemical structure is altered by heating, i.e. charred (Neff et al., 2005). Along with a changing climate, these effects have the power to influence community structure and processes such as soil respiration and nutrient cycling, which can shape future forest C and N cycles on decadal to centurial timescales (Johnstone et al., 2020; Mekonnen et al., 2019). Changing patterns of temperature and precipitation in recent decades have caused increases in frequency, intensity and size of fires across the global boreal region with further amplification predicted in the future (de Groot et al., 2013b; Gillett et al., 2004; Kelly et al., 2013; de Groot et al., 2003). Escalating additions of C to the atmosphere due to fire and changing C cycling in recovering ecosystems may accelerate climate change (Li et al., 2017).

Both long and short term processes have been identified as drivers of the dynamics of fire events. Particularly, the strongest driver of per area emissions of C in boreal wildfires appears to be total fuel (i.e. potentially combustible organic material) which is strongly controlled by long term forest moisture (Walker et al., 2018, 2020). However, in order for this fuel to be available to ignite and sustain fire, it must be both sufficiently dried and spatially arranged to be amenable to high heat and oxygen exposure during an active fire. These factors control fuel availability, the instantaneous proportion of total fuel that is readily combustible. Therefore, boreal wildfire models often incorporate short term fire weather variables (e.g. drought indices, temperature, wind speed, relative humidity) and separate soil fuel loads into distinct compartments such as surface litter, which influences ignition and rate of spread, and the more compactly arranged layers below, which act as a heat reservoir that supports extended smoldering over days to weeks (de Groot et al., 2003; Van Wagner, 1987; Rabin et al., 2017; Kasischke et al., 2005; Wiggins et al., 2020). Composition of tree species, with their associated fire adaptation strategies, has also been shown to have a strong impact on fire severity and intensity and distinguishes the boreal wildfire regimes of the North American and Eurasian continents (Rogers et al., 2015). Furthermore, climate has been observed to have a conditioning effect on fuel chemical composition through its control over vegetation characteristics and the decomposition state of their detrital inputs, which are often represented by the C:N weight ratio in soils (Vanhala et al., 2008; Kohl et al., 2018). Fuel chemical composition, arrangement, moisture content, applied heat and oxygen availability in turn have all been related to the efficiency of the combustion reaction during fire and therefore emission chemistry and the charring of remaining fuel, which can form a surface pyrogenic layer with C and N weight concentrations that differ from the original material (Santín et al., 2016; Dymov et al., 2021; Schmidt and Noack, 2000). Production of charred material is an innately fire driven process and a representative measure

of these interrelated effects. Because additions of char to soils have been observed to have strong impacts on C storage and nutrient cycling (Schmidt and Noack, 2000; Preston and Schmidt, 2006), this fire-induced transformation of remaining fuel is
60 valuable to study alongside its loss from the ecosystem during wildfire.

Boreal C emissions due to a single wildfire can be calculated by multiplying total area burned by estimates of C emissions per area (French et al., 2004; van der Werf et al., 2017). While total area burned may be evaluated directly through remote sensing (Giglio et al., 2018; Ruiz et al., 2012), per area C emissions are generally derived from labor intensive field sampling which is extrapolated to the larger scale either directly or through weighting by remotely sensed data (e.g. topography, vegeta-
65 tion cover, aerosol density) or poorly constrained free parameters such as total fuel load (French et al., 2004; Soja et al., 2004; van der Werf et al., 2017; Veraverbeke et al., 2015; Kaiser et al., 2012). This field sampling has been regionally limited and biased towards a few high intensity burn complexes in North America which may in turn bias global emission estimates (van Leeuwen et al., 2014; Akagi et al., 2011). For example, the Eurasian boreal region is dominated by relatively fire resistant over-
70 story vegetation that avoids excessive heating by promoting lower intensity ground and surface fires than that in boreal North America, which is more prone to spread rapid flaming combustion throughout the canopy (Rogers et al., 2015; de Groot et al., 2013a). C loss due to a group of Siberian boreal forest surface fires was found to be 0.88 kg C m^{-2} (Ivanova et al., 2011) which is about a quarter of what is typical in North American wildfire (3.3 kg C m^{-2}) (Boby et al., 2010; Walker et al., 2020) and about one fifth of an extreme wildfire occurring in Sweden in the year 2014 (4.5 kg C m^{-2}) (Granath et al., 2021). Although Eurasia contains over 70% of the boreal global land area (de Groot et al., 2013a) and about 50% (20 Mha yr^{-1}) of its yearly
75 burnt area (Rogers et al., 2015), methodologies for estimating global and regional C emissions are severely lacking ground validation and meter scale assessments of drivers of C loss variability from this region (van der Werf et al., 2017; Kaiser et al., 2012). Additionally, direct measurements of total N loss from wildfire are rare in all boreal regions despite its well recognized role as a limiting nutrient and evidence of its immediate removal in percentages similar to C (Boby et al., 2010). Lastly, direct field sampling of boreal wildfire has often focused on individual or small groups of fires located relatively near to each other,
80 with little information about the representativeness of the observations or context of the results within the broader spectrum of fire impacts across the wider region, especially those relating to variation in climate. This knowledge gap has thus far been addressed with conglomerated studies spanning different fire seasons, ecosystem types and research methodologies (Walker et al., 2020; Gaboriau et al., 2020). Therefore, widely replicated, simultaneous and systematic field measurements of fire processes in under sampled regions with particular attention to climate are needed to derive more robust, generalizable conclusions
85 about boreal forest responses to wildfire.

This study sampled 50 separate fire complexes spanning broad gradients of mean annual temperature (MAT) and precipitation (MAP) which ignited in Sweden during summer 2018 (Fig. 1). This summer, along with that of 2014, were two of the most extreme fire seasons within Sweden in recent history, driven by severe drought conditions (Wilcke et al., 2020). The goal of this study is to distinguish the effects of climate on fire-induced changes in C and N stocks from an under sampled region with
90 direct, fine scale measurements that both provide insight into local processes and allow for global comparison. Space-for-time substitution (De Frenne et al., 2013) along with a control-impact design provided insight into the possible future conditions of Fennoscandian forests in a changing climate and fire regime. Specifically, it was hypothesized that:

1. Fire significantly reduced C and N stocks across forest compartments.
2. Fire restructured organic layer C and N stocks by increasing overall bulk density and adjusting their weight concentrations across residual compartments and a newly formed pyrogenic layer.
3. Loss of soil and understory C and N stocks and their transfer to the surface pyrogenic layer were correlated to prefire total fuel amount, composition and distribution amongst forest compartments.
4. A direct relation between climate variables and fire-induced C and N stock changes exists.
5. The relation between climate and fire driven C and N stock changes is mediated by long term ecosystem properties that affect the combustion level of forest fuel.

2 Materials and methods

2.1 Experimental design and field site selection

50 burnt plots were selected from a pool of 325 fires identified during the summer 2018 period that had perimeters manually mapped by the Swedish Forest Agency from burn scars appearing in Sentinel-2 infrared data. Each of the $20 \times 20 \text{ m}^2$ plots were located within distinct burn scars (greater than 2 km separation) to reduce potential for pseudoreplication or spatial autocorrelation (Bataineh et al., 2006) and allow for increased spread across the climate gradients (Schweiger et al., 2016). Constraints were placed on plot selection using spatial data within the QGIS (QGIS Development Team, 2019) and ArcGIS (Esri Inc., 2019) software environments. Plot wide values for raster data were taken as the average pixel value within a 20 m diameter circle centered on the plot. The first constraints on site selection were to avoid wetland or steeply sloping areas using prefire, topo-edaphic derived soil moisture data (TEM) provided by the Swedish Environmental Protection Agency (Naturvårdsverket, 2018) and elevation and slope data provided within the ArcGIS software environment. TEM was given as integer values ranging from 0 to 240 and was based on the Soil Topographic Wetness Index (Buchanan et al., 2014) in areas where soil type information was available and on the two topographic indices Depth to Water (Murphy et al., 2007) and the Topographic Wetness Index (Beven and Kirkby, 1979) where soil information was unavailable. This restricted the study to non-wetland ecosystem types, since wetlands tend to have markedly differing ecosystem functioning than relatively drier forested regions, and to retain focus on climate driven effects and their space-for-time substitution by reducing the effects of exogenous variables such as topography on models. Next, sites with postfire salvage logging were omitted using recent visual imagery along with Swedish Forest Agency records. Burnt plot selection was then filtered to maximize the spread over latitude, MAT and MAP gradients. Sentinel-2 infrared imagery was used to locate planned burnt plots near pixels showing the highest intensity within the mapped final burn scar perimeter. This gave greater certainty that the plots experienced a more developed fire effect rather than peripheral heating alone. Otherwise, intensity values were not used to compare separate burn scars. Manual assessment of visual and infrared imagery was performed through the brandkarta web application provided by the Swedish Forest Agency.

In order to estimate the effects of fire, prefire properties of each burnt plot were approximated by measurements from a single identically sized adjacent control plot centered between approximately 15 and 150 m outside the fire boundaries (100 plots total, i.e. 50 plot pairs). A major limitation to this approximation is that observed differences within plot pairs may be skewed through inaccurate or imprecise representation of prefire burnt plot properties by control measurements. An attempt to reduce these errors was made by incorporating a large sample size ($n = 50$) and strict controls on the matching of important ecosystem variables. To reduce mismatch between control and prefire burnt plot properties the following restrictions were placed on control plot selection. Control plot locations were selected to minimize elevation, slope and TEM differences from the adjacent burnt plot. Swedish Forest Agency data regarding tree species, overstory biomass, and basal area (collected during 2014) were used to best match properties of control and burnt plot pairs. Stand appearance and age were examined with historic, visual images provided by the Swedish National Land Survey verifying time since last disturbance had been at least 30 years for plot pairs and that stand structure between plot pairs appeared physically connected over this period.

Due to their documented effects on C emissions (Walker et al., 2018), long and short term approximations of moisture were considered in this study. Long term moisture approximations were separated into a topo-edaphic component (TEM) and climatic component (MAP and MAT). Short term moisture was approximated over the first 6 months of 2018 using the Standardized Precipitation-Evapotranspiration Index (SPEI) with data from the SPEIBase (Beguería et al., 2019) (i.e. spei06 2018-06) to capture the extended desiccation process leading up to each fire. SPEI was also compared to summer 2018 anomalies in temperature and precipitation, i.e. the difference in the 2018 June, July, and August average of these values from those during the same months averaged over the period from 1961 to 2017.

2.2 Sampling

Site visits occurred approximately 1 year postfire over the dates August 5 to August 20 in 2019. This 1 year delay intended to capture the more immediate effects of fire due to potential rapid spikes in nutrient losses and tree mortality, which generally occur within the first year, but avoid the accumulation of discrepancies in C and N stocks relative to control due to any longer term differences in rates of decomposition, leaching and litter addition (Granath et al., 2021; Certini, 2005; Sidoroff et al., 2007). Sampling and analysis were broken into six forest compartments. The compartments included four soil layers, mineral, duff, moss/litter and char, as well as the two aboveground compartments, understory and overstory vegetation, all to be defined in the text below. The organic layer was defined as the duff, moss/litter and char layers grouped together while the soil category was considered as the organic layer grouped with the mineral. The total category refers to the grouping of the soil and understory, but excludes the overstory due to its low observation of combustion (as judged by amounts of canopy blackening). Each compartment was further sorted by weight into sets of characteristic components, here called compartment compositional variables (CCVs), which are to be specifically defined for each compartment in the following sections.

2.2.1 Soil

Soil horizon depths (i.e. the distance from bottom to top of each individual layer) of the mineral, duff, moss/litter, and char layers were measured at 20 points per plot from 10 equally spaced excavations along each plot diagonal (Kristensen et al.,

2015). The mineral layer was measured from its highest rock obstruction to the bottom of the duff layer. The duff layer was considered the conglomerate of the F (partially decomposed material) and H (humic material) layers in accordance with the Canadian system of soil classification (Canada Soil Survey Committee, 1978), as is common in boreal wildfire literature. The moss/litter layer was all unburnt material on top of the duff layer, including visually identifiable detritus and living moss. In all
160 burnt sites, a layer of conglomerated char formed a clear boundary on top of the moss/litter allowing for distinct measurement. Here, char is defined as fully blackened, brittle material with apparent high heat exposure due to fire. This separation was made based on large observed differences in C and N concentrations in surface pyrogenic layers compared to lower residual layers in similar ecosystems (Santín et al., 2016; Dymov et al., 2021; Bodí et al., 2014)

Samples were acquired for all four soil layers. Four mineral soil samples were taken using a 3 cm diameter corer at four
165 corners of a square each 15 m from the plot center. Where feasible, at least 10 cm vertical mineral cores were taken, however in shallower layers a minimum depth of 5 cm each was collected. Duff samples were taken near the mineral cores by excavating four soil volumes, trimming the mineral and moss/litter layers off the bottom and top of the volumes respectively, and then gently cutting right angles with sharp scissors to measure the 3 dimensions in millimeters (collected samples were at least 400 cm³ each). Duff and mineral soils were kept frozen until portions were freeze dried for separate analysis. Moss/litter
170 samples were collected by cutting squares, with attention to preservation of the natural in situ volume, until filling a 553 cm³ steel container. Char layer samples were similarly collected in a 112 cm³ container. At least one sample each of moss/litter and char were acquired from each plot quadrant, though more were taken at equal spacing along a transect to fill the containers if the layer was thin. On the upper surface of the char layer were small portions of dry, unburnt material, which were likely postfire additions of litter to the forest floor. This material was discarded from the char collection and was not included in C
175 and N stock estimates.

2.2.2 Vegetation

Individual tree bole diameter (sampled at 130 cm height above the forest floor) and species were recorded within each plot perimeter for all trees of at least 5 cm diameter at measurement height. A tree was recorded as living if standing upright and having any proportion of green needles (Sidoroff et al., 2007). If a fallen tree was charred only on its lower (in standing ori-
180 entation) portions, it was deemed standing during fire ignition and its measurements were included if its base was within plot boundaries. In burnt plots, the percentage of brown and black needles in each tree canopy was visually approximated as 0%, 25%, 50%, 75%, or 100% with these individual values averaged to give an estimate of total plot canopy browning and blackening. Overstory biomass was calculated by entering bole diameters into allometric equations for Scots pine (*Pinus sylvestris*), Norway spruce (*Picea abies*), silver birch (*Betula pendula*), and downy birch (*Betula pubescens*) (Marklund, 1987). Birch allo-
185 metric equations were applied to the 7 of the 1716 trees sampled in burnt plots that were not one of these 4 species (which were unidentified and deciduous). The equations provided CCVs derived from biomass of stem wood, stem bark, living branches, dead branches, and stump for all species. Roots \geq 5 cm diameter, roots $<$ 5 cm diameter and needle biomass were additionally provided for pine and spruce. Aboveground biomass was considered to be the categories stem wood, stem bark, living branches, dead branches and needles. To form rough estimates of overstory total C and N, C_R for all components was set to

190 0.5 and N_R to 0.01 for needles and 0.004 for all other parts (Boby et al., 2010). Only bole diameters from the burnt plots were used to investigate the influence of overstory vegetation on C and N loss, while bole diameters from adjacent control plots were ignored.

Understory samples were taken from control plots by cutting all non-moss, non-tree plant material at the surface of the soil from within four $40 \times 40 \text{ cm}^2$ patches. To reduce sampling error due to small areal coverage of the plot, the sample patches
195 were chosen by performing transects through the entire plot noting visual estimates of coverage and proportions of plant functional groups (i.e. graminoids, forbs, shrubs, and pteridophytes) which were applied in selecting representative patches for the portion of the plot that was vegetated, which was always all non bare rock surface. These values were applied to a visual estimate of non bare rock surface area of the burnt plots as an approximation of its prefire understory coverage.

2.3 Sample processing

200 All samples were dried at 40°C for at least 3 days. Dry moss/litter samples were weighed and visual estimates for percentage volume of needles, broad leaves, woody material, moss and lichen were multiplied by total weight to form CCVs. This broadly categorized, visual estimation, along with the assumption of equal category density, is meant to test for general effects of variation in proportions of surface fuel types on total soil fuel build up and fire severity. CCVs for understory were determined by sorting the sampled understory plant material and measuring dried weights of the functional groups graminoid, forb, shrub,
205 and pteridophyte. Mineral and duff samples were sieved to 2 mm and 4 mm respectively. The weights of the coarse and fine fractions formed a pair of CCVs for each of the layers. Bulk density of each soil layer per plot was calculated as the total dry weight of its samples divided by their total volume on collection. All samples were pulverized, except the mineral soil where only the fine earth fraction ($< 2 \text{ mm}$) was analyzed (C_R and N_R was set to 0 for the coarse fraction) and packed in tin capsules. The capsules were combusted in a Costech ECS 4010 elemental analyzer, equipped with a 2 m packed chromatographic
210 column for gas separation, to produce ratios of C and N weight to sample total weight (C_R and N_R respectively). After every 10 samples, standardized acetanilide (provided by the company Elemental Microanalysis, Okehampton, United Kingdom) was run to calibrate the machine within 1%. Duff and mineral layer elemental weight ratios were recalculated by the sum of C or N in each of their fine and coarse fractions and divided by total compartment weight. The C:N ratio for each ecosystem compartment was calculated by dividing its total weight of C by total weight N.

215 2.4 Data analysis

The measurable properties used in C and N stock calculations within soil compartments are the depth, bulk density and C_R or N_R . Total C and N stocks per soil compartment were calculated as a product of these properties using the equation

$$\text{Stock}_Z = d \cdot \rho \cdot Z_R \quad (1)$$

where subscript Z is substituted with C or N for reference to C or N stocks, d is the soil layer depth in meters, ρ is the layer
220 bulk density (kg m^{-3}) and Z_R is C_R or N_R . Understory compartment C and N stock calculations were performed with the

equation

$$Stock_Z = \frac{m}{A} \cdot Z_R \cdot F \quad (2)$$

where m is the sampled mass in kilograms, A is sampled area (m^2), Z_R is C_R or N_R , and F is the estimated fractional vegetation coverage of the $20 \times 20 m^2$ plot.

225 Unless otherwise noted, all measured changes between control and burnt plots were first calculated by subtracting control plot values of a variable from those of its burnt pair thereby forming a single distribution of 50 elements for statistical testing. When C and N stocks were described as losses their distribution was negated. These distributions were approximated as normal and all confidence intervals were constructed at the 95% level, unless otherwise noted, using the formula

$$I = \bar{x} \pm z \cdot \frac{\sigma}{\sqrt{n}} \quad (3)$$

230 where \bar{x} is the sample mean, z is always 1.96 for the 95% interval, σ its standard deviation and n the sample size (always 50). Significance of differences between control and burnt plots was deemed to be when their interval did not include zero.

All regression analyses used the ordinary least squares approach to estimate a function for a single response variable based on linear combinations of the predictor variables and an intercept term. Simple regression was performed using the stats.linregress method from SciPy (Virtanen et al., 2020) providing significance (p), correlation (r), and slope (b). Multiple regression was
235 carried out with the OLS method in the Python 3 statsmodels package (Seabold and Perktold, 2010) with models evaluated in order of increasing Akaike information criterion (Akaike, 1974). Standardized regression coefficients (β) were produced by normalizing all variables (i.e. converting to z scores) before regression. All CCVs described in this text were assessed for their direct correlations to C and N stock losses as well as their ability to improve the multiple regression models presented in the results section by using both original variables and their principal components produced by the PCA method in statsmodels.
240 The effects of C and N stock distribution amongst forest compartments were tested by entering the per plot ratios of the sums of different combinations of compartment C and N stocks into regression analyses both directly and to improve all models presented in the results section. Here, variables are considered correlated when p values from simple regression are less than 0.05.

Charting was performed using seaborn (Waskom and the seaborn development team, 2020) and Matplotlib (Hunter, 2007).
245 Bar plot confidence intervals of the mean were bootstrapped at 95% and $n = 10,000$ using the seaborn.barplot method. Additional Python 3 packages that assisted in data exploration were NumPy (Harris et al., 2020) and pingouin (Vallat, 2018).

3 Results

3.1 Survey of burnt plot vegetation

The 50 burn plot overstories were largely dominated by pine with a percentage of spruce stems between 25-50% in 5 plots,
250 between 50-75% in 3 plots and 2 plots with greater than 75%. Birch stems were less than 25% in 44 plots and between 25-50% in 6 plots, of which only 1 of the 6 was spruce dominant. All plots showed visible charring of tree boles though

only 3 plots had greater than 1% plot wide canopy blackening. These plots were pine dominant with 2 having less than 1% spruce while the other had 6 spruce of the 27 stems within the sampled area. Prefire aboveground overstory C and N were estimated as $4.46 \pm 0.738 \text{ kg m}^{-2}$ and $0.0385 \pm 0.00621 \text{ kg m}^{-2}$, respectively, with 5.31% of C ($0.237 \pm 0.0321 \text{ kg m}^{-2}$) and 255 12.3% of N ($0.00474 \pm 0.000641 \text{ kg m}^{-2}$) coming from pine and spruce needles. The 50 burnt plots had a large percentage tree mortality ($45.0 \pm 8.76\%$) compared to control ($4.21 \pm 1.63\%$). Total C and N loss, as well as char layer mass, was not correlated to canopy browning, blackening nor increased mortality in burnt plots relative to control.

Understory coverage was reduced to $10.2 \pm 5.15\%$ of its estimated prefire values. This laid bare the surface layer of charred material present in all plots. This layer was conglomerated and easily separable from lower layers and new litter additions 260 which were mostly needles. Upon breaking apart the layer, it was found to be completely blackened throughout.

3.2 C and N stock losses and restructuring

Averaging across all sites sampled, fire caused significant restructuring of C and N stocks particularly through changing soil depth and bulk density which increased the mass per volume of both C and N. Significant differences in total C stocks in burnt plots from their paired controls were observed, but differences in N were insignificant. Fire clearly converted large amounts 265 of C and N from lower soil layers to the high N_R surface layer of char. Organic layer C_R was unaffected by fire, however strong changes in N_R were measured resulting in an overall significant increase in the C:N ratio of this layer. Mean values and confidence intervals of the differences between control to burnt plots highlighted in this section for all measured compartments are found in Table 1 with soil specific properties found in Table 2.

3.2.1 Total C

270 The largest total loss of C in burnt plot compartments due to fire was from the duff layer (Fig. 2a). About three quarters of the moss/litter C was removed from burnt plots, comprising about half as much as the total amount of C that was removed from the duff layer. Understory C removal due to fire was near complete but had a relatively small contribution to overall C stocks and their changes. Char layer C averaged across the 50 burnt plots was equivalent to 54.3% of the average C lost due to fire from the combined understory and organic compartments. Burnt plot mineral layers had no significant overall change in C between 275 control and burnt plots.

3.2.2 Total N

Fire adjusted the proportions of total N stored in burnt plot forest compartments despite having no overall significant effect on its total amount (Fig. 2b). Similar percentages of N as C were lost from the duff, moss/litter and understory compartments. Char layer N was equivalent to 100.8% of average combined N loss from these combined compartments. Change in N in the 280 mineral layer from control to burnt plots was insignificant.

3.2.3 C:N ratio

The greater proportional reduction of C relative to N from control to burnt plots caused significant decreases in the C:N ratio in all compartments except the duff layer which was unchanged (Fig. 2c). The low C:N ratio in the char layer (29.78 ± 1.70) made a strong contribution to the overall reduction in this value in burnt plot organic layers compared to control.

285 3.2.4 C_R and N_R

The duff layer C_R and N_R did not change significantly, though the moss/litter layer showed a significant increase in both values in burnt plots compared to their paired controls (Fig. 3c, 3d). These layers together with the char layer C_R (0.498 ± 0.0190) and N_R (0.0173 ± 0.00108) resulted in the organic layer having no change in C_R but a significant increase in N_R in burnt plots. The mineral layer had significantly lower C_R and N_R in burnt plots both overall and in the fine fraction C_R (-0.0210 ± 0.0145 ,
290 -33.7%) and N_R (-0.000509 ± 0.000415 , -24.1%) compared to the controls.

3.2.5 Soil layer depths

Fire had a strong effect on reducing soil layer depths with removal of nearly the entire moss/litter layer and about one third of the duff thickness (Fig. 3a). Together with the formation of the char layer and insignificant mineral layer depth changes, fire removed about a quarter of total soil depth and nearly 40% of the organic layer depth in burnt plots. Fire-induced increases in
295 bulk density of the soil layers counteracted C and N loss due to these depth changes (Fig. 3b). Bulk density of both the duff and moss/litter layers increased significantly and, along with producing a dense char layer, fire had a strong densifying effect on the organic layer.

3.2.6 Statistical contribution of measured changes to C and N losses

To quantify the relative statistical contributions of the variation of fire-induced changes in organic layer depth, bulk density
300 and elemental weight ratios, they were used as predictor variables in multiple regression to explain organic layer C and N losses. The C loss regression produced a model of fit of $R^2 = 0.865$ and standardized regression coefficients for changes in depth ($\beta = -0.670$), bulk density ($\beta = -0.633$) and C_R ($\beta = -0.583$). N loss produced a model fit of $R^2 = 0.777$ and coefficients for loss of depth ($\beta = -0.599$), bulk density ($\beta = -0.398$) and N_R ($\beta = -0.382$). This shows that changes of these variables due to fire all had a strong effect on C and N stock loss estimates. Measured change in organic layer depth is the strongest determinant
305 of losses of N. However, for C, bulk density and elemental weight ratios are nearly as important as depth.

3.3 Forest level drivers of fire-induced C and N loss

The strongest correlator to total C and N losses among long term ecosystem properties was total paired control plot C ($p < 0.001$,
 $r = 0.703$, $b = 0.744$) and N stocks ($p < 0.001$, $r = 0.585$, $b = 0.574$), respectively. An even stronger correlation was found between control plot organic layer C and N stocks (here abbreviated C_O and N_O) and estimated losses of C ($p < 0.001$,
310 $r = 0.736$, $b = 0.762$) and N ($p < 0.001$, $r = 0.653$, $b = 0.665$) from this compartment. Due to this increased explanatory power,

and because the majority of fire affected C and N stocks were located there, the focus of analysis was placed on the organic layer. Variables used in regression with percentage changes in C and N stocks tended to have less explanatory power than total C and N stock losses and also were sensitive to outliers having erratic changes in model fit with removal of data points. Therefore only total C and N stock losses were assessed.

315 The interaction effect of C_O and N_O (i.e. its C:N ratio) was added to improve model fit. C_O and its C:N ratio strongly explained C_O losses ($p < 0.001$, $R^2 = 0.588$) while N_O and its C:N ratio explained N_O losses with slightly less strength ($p < 0.001$, $R^2 = 0.519$). Multicollinearity between the organic layer C:N ratio and C_O ($p = 0.003$, $r = -0.411$, $b = -1.96 \text{ kg C m}^{-2}$) and N_O ($p < 0.001$, $r = -0.578$, $b = -92.2 \text{ kg N m}^{-2}$) did not produce a high condition number in these models (1.55 for C, 1.93 for N) suggesting they are robust to these covariations (Alin, 2010).

320 Total char layer C was not significantly related to loss of C_O ($p = 0.137$) however a significant correlation using simple regression was found between char layer N and losses of N_O ($p = 0.011$, $r = -0.359$, $b = -0.838$).

CCVs and distribution of C and N stocks amongst control plot compartments could not improve these models explaining C_O and N_O losses in multiple regression with C_O and N_O respectively nor could they significantly explain the build up of organic layer fuel in control plots or production of char C or N. Relations either did not suitably meet the basic assumptions of regression, were deemed to be confounding or lacked supporting causal mechanism and were at a high risk of omitted-variable bias.

3.4 Climatic drivers of fire-induced C and N loss

MAP had a directly proportional relation to both C_O ($p < 0.001$, $R^2 = 0.465$, $b = 0.0194 \text{ kg C m}^{-2} \text{ mm}^{-1}$) and N_O ($p = 0.012$, $R^2 = 0.352$, $b = 0.000416 \text{ kg N m}^{-2} \text{ mm}^{-1}$) losses. In multiple regression, MAT and MAT² formed a negative quadratic relation to losses in C_O ($p = 0.008$, $R^2 = 0.186$) and N_O ($p = 0.002$, $R^2 = 0.233$), both peaking near 4 °C. In multiple regression of the 3 variables the MAT and MAT² terms lost significance and MAP was the dominant explaining factor of C_O and N_O losses. MAT and MAP were not significantly related in simple regression ($p = 0.829$) however a negative quadratic function of MAT in multiple regression explained MAP ($p < 0.001$, $R^2 = 0.407$), again peaking near 4 °C. This suggests that the direct climate dependence of C_O and N_O losses were driven by MAP, with MAT relating indirectly through its association to MAP.

Control plot C_O and N_O were broken down into the three measured aspects of depth, bulk density, and elemental weight ratio and entered as a linear combination in multiple regression within path analyses (Fig. 4a, b). MAT and MAP enhanced fire-induced C_O and N_O loss by promoting development of a denser, more voluminous fuel load with additional direct effects on losses by MAT. MAT mitigates C_O loss by reducing C_R , however variation in this value does not affect C_O loss as strongly as depth and bulk density. Conversely, MAT promotes N_O loss through a higher N_R fuel but exerts a stronger direct effect on reduction of N_O removal due to fire than in the C_O model. Accordingly, a separate multiple regression showed strong negative effects of MAT and MAP on organic layer C:N ratio (Fig. 5a) along with a direct effect of MAT ($p < 0.001$, $r = -0.568$, $b = -2.50 \text{ °C}^{-1}$). CCVs could not strongly link MAT or MAP with C_R , N_R , or the C:N ratio in control plot organic layers.

Total char layer mass ($p < 0.001$, $r = 0.453$, $b = 0.316 \text{ kg m}^{-2} \text{ }^\circ\text{C}^{-1}$) and char C_R ($p = 0.002$, $r = -0.435$, $b = -0.012 \text{ }^\circ\text{C}^{-1}$) were correlated with MAT but not the total mass of prefire fuel. This means that warmer regions produced larger amounts of lower C_R material irrespective of total fuel amount. In a multiple regression using C_O , the organic layer C:N ratio, MAT, MAP and total char layer C production to explain C_O loss, direct effects of MAT lost significance and overall model fit was improved (Fig. 5a). This suggested that, while controlling for C_O and the organic layer C:N ratio, C_O loss from this layer was reduced by MAT through the creation of char. Similarly, N_O loss is further explained by additions of char layer N to the climate model but a large direct effect of MAT remains (Fig. 5b). The organic layer C:N ratio in the N model was able to replace the direct effect of MAT, however with decreased model fit and inflation of variables which is suggestive of a confounding influence of the organic layer C:N ratio on MAT and N_O loss. Again, CCVs and fuel distribution could not improve either model.

3.5 Moisture and summer 2018 anomalies

TEM was not directly related to C_O ($p = 0.248$) or N_O ($p = 0.259$) stocks in control plots though it slightly improved model fit when joined with MAT and MAP in explaining these variables (Fig. 5a, b). TEM differences between paired burnt and control plots were observed to increase both with control and burnt TEM levels however not along gradients of MAT ($p = 0.198$), MAP ($p = 0.771$), C_O ($p = 0.302$) or N_O ($p = 0.423$). TEM differences between paired burnt and control plots were entered into simple regression with losses in C_O ($p = 0.088$, $r = -0.244$, $b = -0.0132 \text{ kg C m}^{-2}$) and N_O ($p = 0.035$, $r = -0.299$, $b = 0.00415 \text{ kg N m}^{-2}$). Although, correction for these slopes by using non-standardized coefficients of regression for TEM, MAT and MAP against C_O and N_O produced no significant change in losses of C_O or N_O .

SPEI was related to MAT ($p < 0.001$, $r = -0.869$), temperature anomaly ($p < 0.001$, $r = -0.892$), precipitation anomaly ($p = 0.002$, $r = -0.433$) but not to MAP ($p = 0.725$), or losses of C_O ($p = 0.712$) and N_O ($p = 0.644$) due to fire. When included in multiple regression with MAP, MAT, char C or N, and C_O or N_O to explain fire-induced C_O or N_O stock losses, respectively, SPEI either did not improve model fit or promoted high uncertainty of variables. SPEI was directly related to char C ($p = 0.013$, $r = -0.348$) and N ($p = 0.012$, $r = -0.351$) but had high uncertainty when explaining these variables in multiple regression with MAT which suggests SPEI is a confounding variable. Additionally, anomalies of temperature ($p < 0.001$, $r = 0.956$) and precipitation ($p < 0.001$, $r = -0.525$) were strongly correlated to their respective long term values with the temperature anomaly offering improved explanation of total char production ($p < 0.001$, $r = 0.477$, $b = 0.179 \text{ kg m}^{-2} \text{ }^\circ\text{C}^{-1}$) over MAT.

4 Discussion

4.1 Trends in ecosystem C and N stocks

Significant overall reduction in C stocks were found in burnt plots relative to their paired control, with the largest removals from the duff layer. Averaged total C loss was relatively low at $0.815 \pm 0.652 \text{ kg C m}^{-2}$ (15.6%) compared to estimates from inland Alaskan black spruce stands (3.3 kg C m^{-2}) (Boby et al., 2010) but was comparable to averaged losses from Scots pine stands in Siberia ($0.992 \text{ kg C m}^{-2}$) (Ivanova et al., 2011). A single, exceptionally large wildfire occurring in Sweden in

375 2014 released an estimated 4.50 kg C m^{-2} (Granath et al., 2021) which lies just above the 93rd percentile of C loss estimates within the 50 plot network of the current study. Unlike C, however, N stocks were not significantly different overall in burnt plots compared to controls. This contrasts with the Alaskan study which estimated percentage removal from soils of N (49.8%) to be similar to C (52.9%) at an average loss of 0.09 kg N m^{-2} (Boby et al., 2010). Averaging over the 50 burnt plots, fire clearly reduced N in large amounts within the residual duff and moss/litter layers but captured it within the high N_R char layer, preventing differences when considering the overall soil profile. Proximity to the soil surface suggest a portion of the char layer was likely always derived from fire interacting with the understory and moss/litter layer, however averaged char layer C and N stocks were greater than losses from the two layers combined suggesting there were large contributions also from the duff. In burnt plots with residual moss/litter an upwards mixing of mobilized duff C and N (e.g. in the form of volatiles or soot) may have occurred due to simultaneous heating throughout the depth of the fuel bed. Because the char layer was conglomerated and completely blackened, it is unlikely that material was incorporated postfire. However, material may have been added from downward movement of overstory components during the time of fire or deposition of aerosols coming from outside the plot. By selecting plots well within the final fire perimeter it was assumed that incoming and outgoing aerosols during the fire would be approximately equal and that extended aerosol deposition from more remote sources would accumulate equally on control and burnt plots. The above mentioned study in Alaskan black spruce forests, which are known for their great extent of canopy damage (Walker et al., 2020; Boby et al., 2010), showed C and N loss from the canopy to be about an order of magnitude lower than losses from soil while also assuming that losses from the tree bole are negligible and that a large fraction of these overstory losses were released to the atmosphere (Boby et al., 2010). An experimental high intensity crown fire in a Canadian jack pine forest with relatively low soil C stores (1.97 kg C m^{-2}) had minimal C losses from tree boles at 0.08 kg C m^{-2} , though needle C losses were substantial at 0.51 kg C m^{-2} (94.4% needle C) (Santín et al., 2015). In the current study, despite a substantial portion of C and N stored in needles, low levels of overstory blackening and its lack of correlation with char layer mass suggests that the large majority of C and N stock changes between control and burnt plots were captured within the sampled soil and understory compartments.

The lack of change in total N stock due to fire is consistent with available evidence from existing study in Fennoscandian forests where fire had only slight effects on total N over extended periods (Palviainen et al., 2017). N losses in non-boreal forests have been related to fire temperature during time of fire with lower intensity fires transferring a greater proportion of pools of organic N into soil ammonium and nitrate rather than removing N in gaseous forms (Neary et al., 1999). Laboratory studies have linked the amount of N transferred from organic to inorganic forms during heat exposure to both applied temperature and fuel type (Gundale and DeLuca, 2006; Makoto et al., 2011). Therefore, the N cycle in boreal systems may be highly dependent on active fire properties, fuel type and resulting fuel transformation and the greater N losses in Alaska compared to Eurasia could be explained by its dissimilar fuel and the characteristically more intense crown fires across the North American boreal zone (de Groot et al., 2013a; Wooster and Zhang, 2004). Fire intensity and temperature have also been linked to both C and overall fuel transformation in experimental forest fire (Santín et al., 2016), so it is of interest to compare remote measurements (i.e. satellite data) of these time-of-fire properties to on-site measured ecosystem changes. This can lead to a more complete predictive understanding of wildfire in the entire Fennoscandian region and beyond.

410 In addition to removals, C and N were densified by fire in the organic layers due to their significant drops in depth and increased bulk density in burnt plots. The lower mean C_R in burnt plot organic layers relative to control is assumed to be due to the increased ratio of remaining incombustible material to remaining organic material. However, large variability of duff C_R in burnt plots contributed to the statistical insignificance of this change and appeared to be related to extreme volume reductions which reduced the duff layer to exceptionally ashy, rocky material in some plots. The large, significant increase in
415 N_R in the organic layer can be attributed to the formation of the high N_R char layer. The strong alteration of char layer C:N relative to prefire fuel is comparable to results from studies that have incorporated similar pyrogenic layers that are observed to be a mixture of organic or inorganic material types across broad ranges of combustion completeness (Bodí et al., 2014). For example, the C:N ratio in a pyrogenic layer 1 year after a low intensity Siberian Larch forest surface fire in Russia was 31.4 (prefire 49.1), which is much lower than the 43.8 C:N ratio (prefire 39.4) observed the day after an experimental, high
420 intensity jack spruce crown fire in Canada (Santín et al., 2016; Dymov et al., 2021), further suggesting general differences in thermolability of soil C and N under regionally varied characteristic heating regimes.

Fire-induced morphological change of fuel has been shown to play a strong role in N retention where highly porous char material adsorbs inorganic N preventing its leaching loss from the system until its reuptake into organic forms by plants or microbes (Makoto et al., 2012). This sorptive power has been observed to fade over the interval between fire events suggesting
425 newly produced char is required for this retention effect (Zackrisson et al., 1996). The high N_R of the char layer may therefore be due in part to adsorption of fire mineralized N or preserved, prefire mineral N and act as a steady source of bioavailable nutrients to plant and microbial communities during succession. In addition, N may be stored in this layer in partially combusted or depolymerized organic forms (Certini, 2005). This study employed coarse-scale sampling of char based on soil horizon identification with separation in the field and a more rigorously defined assessment of char production in all layers may provide
430 further detail relating it to climate and soil processes.

4.2 Climate linked effects of fire

Both MAP and MAT had significant direct relations to total C and N removals from plots with the strongest mediator being estimated prefire C and N stocks in the organic layer. MAP had a stronger effect on the build up of control plot fuel, namely through a positive correlation with total organic layer depth. MAT affected C and N losses through increasing bulk density,
435 reducing C_R and increasing N_R thus reducing the C:N ratio in the organic layer in control plots, suggesting warmer conditions had a fuel conditioning effect through greater decomposition of organic soils (Callesen et al., 2007). When controlling for control plot organic layer C and N stocks and their ratios using multiple regression, MAT had a direct negative effect on C and N losses from this layer. This direct effect was largely mediated by the incorporation of measures of fire-induced fuel transformation into the models, i.e. production of char layer C or N. These models suggest that warmer regions tended to
440 conserve larger pools of fire affected fuel as charred material rather than release it from the ecosystem either in gaseous, particulate or dissolved forms over the 1 year postfire period. This fuel restructuring in turn may have extended effects on C and N turnover through links to nutrient availability and the biotic community which in turn affect process rates such as primary production and soil decomposition (Schmidt and Noack, 2000).

4.3 Considering representativeness and prediction of future wildfire impacts

445 A caveat of the pair plot matching methodology is that burnt plots may have had a greater tendency to ignite due to specific properties that heighten their fire susceptibility relative to controls. As a result, the comparably low C and N losses may be due to underestimation via burnt plots being biased to a greater prefire fuel load than their paired controls (systematic error) rather than these differences being approximately random (random error). This was evident in the fact that N losses were centered near 0 by their mean yet had a strong correlation with control plot total N despite the improbability that fire actually
450 increased total N within nearly half of the burnt plot sample pool. Contrarily, control plots were biased towards higher TEM, which was observed to be related to greater fuel loading in measured control plots, though the magnitude of this bias did not increase along gradients of climate or fuel loading nor did attempts to correct for it significantly affect C and N loss estimates. Therefore, control plot matching appears to have been performed adequately within the scope of data collected, with any potential bias coming from unknown parameters. Further investigation of these unknowns is merited in order to improve
455 control plot matching methodology and better constrain emission estimates in this region.

Further support of trends identified within the pair plot methodology was provided by separating analysis of the pyrogenic char layer, which was unique to burnt plots, from the soil profile as a whole. The large shifts in N_R and the C:N ratio in the char layer relative to lower layers in burnt plots show a clear preferential removal of C relative to N due to fire. This C:N ratio reduction was opposite to the C:N increases observed in a pyrogenic layer in more intense North American crown fire,
460 which may be due to differences in fire temperature and heating duration (Santín et al., 2016). Therefore, until more predictive knowledge is gained over the proportional losses of C and N, accurate estimates of their stock changes due to fire may require measurements of densities of these individual elements throughout the residual soil profile in burnt plots.

Variation of many ecosystem properties could not be statistically linked to C and N losses, though that does not mean they are without role in determining extent of emissions and ecosystem change. Cross regional boreal wildfire study has shown variables
465 such as the abundance of spruce to strongly affect C emissions across regions, but within a single region the abundance may be too homogeneous to show an effect (Walker et al., 2020). Furthermore, ratios of fine to heavy fuel loads have been manipulated in experimental burns to produce varying fire severity (Alexander et al., 2018; Ludwig et al., 2018). Accordingly, CCVs and fuel distribution amongst compartments in this study may have been simply too homogeneous to produce significant results but may nevertheless still provide valuable statistical signals for understanding drivers of fire processes across regions and fire
470 severities.

Previous studies have demonstrated strong effects of moisture on boreal wildfire C emissions. For example, a study including several large North American fire complexes found C emissions to increase along gradients of topo-edaphic derived soil moisture (due to its positive relation to total fuel) until reaching high moisture sites where the trend inverted and began to decrease due to the inhibiting effects of this increased moisture on fuel availability (Walker et al., 2018). The position of this point of
475 inflection along the long term moisture curve is likely dictated by short term moisture levels, which are in turn controlled by the extremity of drying during a fire season. Accordingly, fuel availability, and therefore C emissions, are strongly dependent on drying processes specific to individual stand composition and structure and its local fire weather. By incorporating measures

of long (TEM, MAT, MAP) and short term moisture balance (SPEI), climate based path models gained only slight improvements in explaining fuel build up and no increased explanatory power regarding C and N losses. Therefore, the study design distinguished climate driven effects on fire severity with only minimal restrictions on site selection (non-sloping, non-wetland) thereby providing results that are generally representative for Fennoscandian, non-wetland forests under similar drought conditions of summer 2018. However, with its strong correlations to drought indices, anomalies of temperature and precipitation as well as fuel charring and remaining direct effects on emissions, more remains to be understood about how MAT (and in addition, intra-annual distribution of MAP) relates to the fire regime across the conditions of different fire seasons.

Fuel loading has been found to have a varied strength of control on boreal wildfire C loss globally. This study found total C loss to relate to belowground C in simple regression with an R^2 of 0.494 and to aboveground C insignificantly. These results are within the broad range found in Walker et al. (2020) where total C losses across 4 North American boreal ecoregions were directly related to prefire belowground C with R^2 values of 0.024 (insignificant), 0.07, 0.051, and 0.579 and to respective prefire aboveground C with R^2 values of 0.229, 0.005 (insignificant), 0.101, and 0.336. Little is known about which factors dictate the strength of these controls and what portions of unexplained variation can be attributed to either additional measurable factors, methodological error or stochastic fire processes for a particular wildfire event. This study attempted to address these issues by testing many measurable ecosystem properties across several ecosystem C storage compartments finding the organic layer C stock along with its climate related prefire fuel conditioning and combustion susceptibility to be most predictive of C loss (Fig. 4a). These trends were demonstrated using a consistent methodology that incorporates high replication and broad spatial coverage, thereby offering better constraints on remaining unexplained variation across the region than might be provided by sampling a single burn scar or comparing results from different study designs.

Boreal wildfire literature has tended to focus on highly flammable forest ecosystems with intense burning of several hundred hectares or more despite the vast majority of fires in the boreal region being less than 200 ha (Stocks et al., 2002; Valendik, 1996). This research bias may limit knowledge to a particular population by studying fire events only at their utmost extremes and effectively masking important signals of ecosystem heterogeneity on fire severity at differing intensities. The only restriction this study placed on wildfire intensity and size was that the fire activity could be remotely confirmed using Sentinel-2 infrared data. This has the potential to affect comparability of results both in terms of total C and N losses as well as their drivers which may exhibit differing patterns and strengths over ranges of fire intensity. It may therefore be beneficial for wildfire studies to be examined and compared within categories of absolute severity and intensity. This methodology might be particularly useful in gaining understanding of the drivers of fire severity as it increases in traditionally fire protected ecosystems such as wetlands (Zoltai et al., 1998), which tend to store vastly larger amounts of C per area than their dryer forested counterparts in the boreal region (Deluca and Boisvenue, 2012).

5 Conclusions

This study measured wildfire impacts across current climatic gradients of precipitation and temperature to show that climate controls total releases of C and N during fire events mainly due to its effect on increasing organic layer fuel load. The role of

MAP is focused on the total quantity of this fuel load whereas MAT has a more qualitative effect by influencing bulk density, C_R and N_R in the organic layer. When controlling for total organic layer fuel, increasing MAT, and to a lesser extent MAP, reduces C loss due to fire through preconditioning of the organic layer as measured by a lowered C:N ratio. Additionally, both C and N losses are mitigated by increased MAT through the sequestering of fire affected fuel into a surface layer of charred material.

515 This conservation effect is stronger for N, which had no overall significant loss in stocks due to fire, and which also had stronger unexplained direct mitigating effects of MAT on its loss that were hypothesized to be related to time-of-fire properties such as fire intensity and temperature. While remaining ecosystem variables regarding fuel composition and distribution could not be strongly linked to total C and N losses it is of interest to analyze their role in cross-regional comparisons and to investigate whether they influence other fire related properties such as ignition likelihood, fire propagability and intensity. Advancing

520 knowledge of the intricate ties between instantaneous processes of fire events and their long term effects on C and N cycling demands comprehensive research approaches that pay particular attention to climate sensitivity. This knowledge is imperative for producing accurate predictions of boreal forest functioning under future climate scenarios.

Data availability. All data used to produce the results in this document are original unless otherwise stated in the text. It is found freely available through Eckdahl et al. (2021).

525 *Author contributions.* Author contributions using the CRediT contributor roles taxonomy are as follows: conceptualization (JAE, JAK, DBM), data curation (JAE), formal analysis (JAE), funding acquisition (JAK, DBM), investigation (JAE, JAK, DBM), methodology (JAE, JAK, DBM), project administration (JAE, JAK, DBM), resources (JAE, DBM), software (JAE), supervision (JAE, JAK, DBM), validation (JAE, JAK, DBM), visualization (JAE), writing – original draft preparation (JAE), and writing – review & editing (JAE, JAK, DBM).

Competing interests. The authors declare that they have no conflict of interest.

530 *Acknowledgements.* JAE was supported by the strategic research area Biodiversity and Ecosystems in a Changing Climate, BECC, at Lund University. JAK was supported by the Carlsberg Foundation (grant CF20-0238). C and N analyses were performed in the Department of Geology, Lund University under supervision of Karl Ljung. Valuable information was provided by representatives from the Swedish Forest Agency (Skogsstyrelsen) and Swedish Civil Contingencies Agency (Myndigheten för samhällsskydd och beredskap, MSB). Thank you to Geerte de Jong for dedicated assistance in field work planning and execution. Crucial field and lab assistance was provided by Rieke Madsen,

535 Femke Pijcke, Lotte Wendt, Julia Iwan, and Henni Yläne. Guidance from Karl Ljung, Åsa Wallin, Patrik Vestin and Michael Gundale in sample collection and processing was critical and highly appreciated. Thanks are given to two anonymous reviewers who provided helpful suggestions for improvement during manuscript development. Friends, family, and colleagues were vital sources of support and inspiration throughout this work.

References

- 540 Akagi, S. K., Yokelson, R. J., Wiedinmyer, C., Alvarado, M. J., Reid, J. S., Karl, T., Crouse, J. D., and Wennberg, P. O.: Emission factors for open and domestic biomass burning for use in atmospheric models, *Atmospheric Chemistry and Physics*, 11, 4039–4072, <https://doi.org/10.5194/acp-11-4039-2011>, 2011.
- Akaike, H.: A new look at the statistical model identification, *IEEE Transactions on Automatic Control*, 19, 716–723, <https://doi.org/10.1109/TAC.1974.1100705>, 1974.
- 545 Alexander, H. D., Natali, S. M., Loranty, M. M., Ludwig, S. M., Spektor, V. V., Davydov, S., Zimov, N., Trujillo, I., and Mack, M. C.: Impacts of increased soil burn severity on larch forest regeneration on permafrost soils of far northeastern Siberia, *Forest Ecology and Management*, 417, 144–153, <https://doi.org/10.1016/j.foreco.2018.03.008>, 2018.
- Alin, A.: Multicollinearity, *WIREs Computational Statistics*, 2, 370–374, <https://doi.org/10.1002/wics.84>, 2010.
- Bataineh, A. L., Oswald, B. P., Bataineh, M., Unger, D., Hung, I.-K., and Scognamillo, D.: Spatial autocorrelation and pseudoreplication in
550 fire ecology, *Fire Ecology*, 2, 107–118, <https://doi.org/10.4996/fireecology.0202107>, 2006.
- Beguería, S., Latorre, B., Reig, F., and Vicente-Serrano, S. M.: Global SPEI database, <https://spei.csic.es/database.html>, 2019.
- Beven, K. J. and Kirkby, M. J.: A physically based, variable contributing area model of basin hydrology, *Hydrological Sciences Bulletin*, 24, 43–69, <https://doi.org/10.1080/02626667909491834>, 1979.
- Boby, L. A., Schuur, E. A. G., Mack, M. C., Verbyla, D., and Johnstone, J. F.: Quantifying fire severity, carbon, and nitrogen emissions in
555 Alaska's boreal forest, *Ecological Applications*, 20, 1633–1647, <https://doi.org/10.1890/08-2295.1>, 2010.
- Bodí, M. B., Martín, D. A., Balfour, V. N., Santín, C., Doerr, S. H., Pereira, P., Cerdà, A., and Mataix-Solera, J.: Wildland fire ash: Production, composition and eco-hydro-geomorphic effects, *Earth-Science Reviews*, 130, 103–127, <https://doi.org/https://doi.org/10.1016/j.earscirev.2013.12.007>, 2014.
- Bond-Lamberty, B., Peckham, S. D., Ahl, D. E., and Gower, S. T.: Fire as the dominant driver of central Canadian boreal forest carbon
560 balance, *Nature*, 450, 89–92, <https://doi.org/10.1038/nature06272>, 2007.
- Buchanan, B. P., Fleming, M., Schneider, R. L., Richards, B. K., Archibald, J., Qiu, Z., and Walter, M. T.: Evaluating topographic wetness indices across central New York agricultural landscapes, *Hydrology and Earth System Sciences*, 18, 3279–3299, <https://doi.org/10.5194/hess-18-3279-2014>, 2014.
- Callesen, I., Raulund-Rasmussen, K., Westman, C., and Tau-Strand, L.: Nitrogen pools and C:N ratios in well-drained Nordic forest soils
565 related to climate and soil texture, *Boreal Environment Research*, 12, 681–692, 2007.
- Canada Soil Survey Committee: The Canadian system of soil classification, Research Branch, Canada Department of Agriculture, 1978.
- Certini, G.: Effects of fire on properties of forest soils: a review, *Oecologia*, 143, 1–10, <https://doi.org/10.1007/s00442-004-1788-8>, 2005.
- De Frenne, P., Graae, B. J., Rodríguez-Sánchez, F., Kolb, A., Chabrerie, O., Decocq, G., De Kort, H., De Schrijver, A., Diekmann, M., Eriksson, O., Gruwez, R., Hermy, M., Lenoir, J., Plue, J., Coomes, D. A., and Verheyen, K.: Latitudinal gradients as natural laboratories
570 to infer species' responses to temperature, *Journal of Ecology*, 101, 784–795, <https://doi.org/10.1111/1365-2745.12074>, 2013.
- de Groot, W., Bothwell, P., Carlsson, D., and Logan, K.: Simulating the effects of future fire regimes on western Canadian boreal forests, *Journal of Vegetation Science*, 14, 355–364, <https://doi.org/10.1111/j.1654-1103.2003.tb02161.x>, 2003.
- de Groot, W. J., Cantin, A. S., Flannigan, M. D., Soja, A. J., Gowman, L. M., and Newbery, A.: A comparison of Canadian and Russian boreal forest fire regimes, *Forest Ecology and Management*, 294, 23–34, <https://doi.org/10.1016/j.foreco.2012.07.033>, 2013a.

- 575 de Groot, W. J., Flannigan, M. D., and Cantin, A. S.: Climate change impacts on future boreal fire regimes, *Forest Ecology and Management*, 294, 35–44, <https://doi.org/10.1016/j.foreco.2012.09.027>, 2013b.
- DeLuca, T. H. and Boisvenue, C.: Boreal forest soil carbon: distribution, function and modelling, *Forestry*, 85, 161–184, <https://doi.org/10.1093/forestry/cps003>, 2012.
- Dymov, A., Startsev, V., Milanovsky, E., Valdes-Korovkin, I., Farkhodov, Y., Yudina, A., Donnerhack, O., and Guggenberger, G.: Soils and
580 soil organic matter transformations during the two years after a low-intensity surface fire (Subpolar Ural, Russia), *Geoderma*, 404, 115 278, <https://doi.org/https://doi.org/10.1016/j.geoderma.2021.115278>, 2021.
- Eckdahl, J., Kristensen, J., and Metcalfe, D.: Dataset for Boreal Forest Wildfire and Climate Linked Drivers of Carbon and Nitrogen Loss, <https://doi.org/10.5281/zenodo.5078669>, 2021.
- Esri Inc.: ArcGIS Pro, Esri Inc., <https://www.esri.com/en-us/arcgis/products/arcgis-pro/>, 2019.
- 585 French, N. H., Goovaerts, P., and Kasischke, E. S.: Uncertainty in estimating carbon emissions from boreal forest fires, *Journal of Geophysical Research: Atmospheres*, 109, <https://doi.org/10.1029/2003JD003635>, 2004.
- Gaboriau, D. M., Remy, C. C., Girardin, M. P., Asselin, H., Hély, C., Bergeron, Y., and Ali, A. A.: Temperature and fuel availability control fire size/severity in the boreal forest of central Northwest Territories, Canada, *Quaternary Science Reviews*, 250, 106 697, <https://doi.org/10.1016/j.quascirev.2020.106697>, 2020.
- 590 Giglio, L., Boschetti, L., Roy, D. P., Humber, M. L., and Justice, C. O.: The Collection 6 MODIS burned area mapping algorithm and product, *Remote Sensing of Environment*, 217, 72–85, <https://doi.org/10.1016/j.rse.2018.08.005>, 2018.
- Gillett, N., Weaver, A., Zwiers, F., and Flannigan, M.: Detecting the effect of climate change on Canadian forest fires, *Geophysical Research Letters*, 31, <https://doi.org/10.1029/2004GL020876>, 2004.
- Granath, G., Evans, C. D., Strengbom, J., Fölster, J., Grelle, A., Strömqvist, J., and Köhler, S. J.: The impact of wildfire on biogeochemical
595 fluxes and water quality in boreal catchments, *Biogeosciences*, 18, 3243–3261, <https://doi.org/10.5194/bg-18-3243-2021>, 2021.
- Gundale, M. J. and DeLuca, T. H.: Temperature and source material influence ecological attributes of ponderosa pine and Douglas-fir charcoal, *Forest ecology and management*, 231, 86–93, <https://doi.org/10.1016/j.foreco.2006.05.004>, 2006.
- Harris, C. R., Millman, K. J., van der Walt, S. J., Gommers, R., Virtanen, P., Cournapeau, D., Wieser, E., Taylor, J., Berg, S., Smith, N. J., Kern, R., Picus, M., Hoyer, S., van Kerkwijk, M. H., Brett, M., Haldane, A., Fernández del Río, J., Wiebe, M., Peterson, P., Gérard-
600 Marchant, P., Sheppard, K., Reddy, T., Weckesser, W., Abbasi, H., Gohlke, C., and Oliphant, T. E.: Array programming with NumPy, *Nature*, 585, 357–362, <https://doi.org/10.1038/s41586-020-2649-2>, 2020.
- Hunter, J. D.: Matplotlib: A 2D graphics environment, *Computing in Science & Engineering*, 9, 90–95, <https://doi.org/10.1109/MCSE.2007.55>, 2007.
- Ivanova, G., Conard, S., Kukavskaya, E., and McRae, D.: Fire impact on carbon storage in light conifer forests of the Lower Angara region,
605 Siberia, *Environmental Research Letters*, 6, 045 203, <https://doi.org/10.1088/1748-9326/6/4/045203>, 2011.
- Johnstone, J., Celis, G., Chapin III, F., Hollingsworth, T., Jean, M., and Mack, M.: Factors shaping alternate successional trajectories in burned black spruce forests of Alaska, *Ecosphere*, 11, e03 129, <https://doi.org/10.1002/ecs2.3129>, 2020.
- Kaiser, J. W., Heil, A., Andreae, M. O., Benedetti, A., Chubarova, N., Jones, L., Morcrette, J.-J., Razinger, M., Schultz, M. G., Suttie, M., and van der Werf, G. R.: Biomass burning emissions estimated with a global fire assimilation system based on observed fire radiative
610 power, *Biogeosciences*, 9, 527–554, <https://doi.org/10.5194/bg-9-527-2012>, 2012.

- Kasischke, E. S., Hyer, E. J., Novelli, P. C., Bruhwiler, L. P., French, N. H., Sukhinin, A. I., Hewson, J. H., and Stocks, B. J.: Influences of boreal fire emissions on Northern Hemisphere atmospheric carbon and carbon monoxide, *Global Biogeochemical Cycles*, 19, <https://doi.org/10.1029/2004GB002300>, 2005.
- 615 Keenan, R. J., Reams, G. A., Achard, F., de Freitas, J. V., Grainger, A., and Lindquist, E.: Dynamics of global forest area: Results from the FAO Global Forest Resources Assessment 2015, *Forest Ecology and Management*, 352, 9–20, <https://doi.org/10.1016/j.foreco.2015.06.014>, 2015.
- Kelly, R., Chipman, M. L., Higuera, P. E., Stefanova, I., Brubaker, L. B., and Hu, F. S.: Recent burning of boreal forests exceeds fire regime limits of the past 10,000 years, *Proceedings of the National Academy of Sciences*, 110, 13 055–13 060, <https://doi.org/10.1073/pnas.1305069110>, 2013.
- 620 Kohl, L., Philben, M., Edwards, K. A., Podrebarac, F. A., Warren, J., and Ziegler, S. E.: The origin of soil organic matter controls its composition and bioreactivity across a mesic boreal forest latitudinal gradient, *Global Change Biology*, 24, e458–e473, <https://doi.org/10.1111/gcb.13887>, 2018.
- Kristensen, T., Ohlson, M., Bolstad, P., and Nagy, Z.: Spatial variability of organic layer thickness and carbon stocks in mature boreal forest stands—implications and suggestions for sampling designs, *Environmental monitoring and assessment*, 187, 1–19, <https://doi.org/10.1007/s10661-015-4741-x>, 2015.
- 625 Lemprière, T., Kurz, W., Hogg, E., Schmoll, C., Rampley, G., Yemshanov, D., McKenney, D., Gilsean, R., Beatch, A., Blain, D., Bhatti, J., and Krmar, E.: Canadian boreal forests and climate change mitigation, *Environmental Reviews*, 21, 293–321, <https://doi.org/10.1139/er-2013-0039>, 2013.
- Li, F., Lawrence, D. M., and Bond-Lamberty, B.: Impact of fire on global land surface air temperature and energy budget for the 20th century due to changes within ecosystems, *Environmental Research Letters*, 12, 044 014, <https://doi.org/10.1088/1748-9326/aa6685>, 2017.
- 630 Ludwig, S. M., Alexander, H. D., Kielland, K., Mann, P. J., Natali, S. M., and Ruess, R. W.: Fire severity effects on soil carbon and nutrients and microbial processes in a Siberian larch forest, *Global Change Biology*, 24, 5841–5852, <http://dx.doi.org/10.1111/gcb.14455>, 2018.
- Makoto, K., Choi, D., Hashidoko, Y., and Koike, T.: The growth of *Larix gmelinii* seedlings as affected by charcoal produced at two different temperatures, *Biology and Fertility of Soils*, 47, 467–472, <https://doi.org/10.1007/s00374-010-0518-0>, 2011.
- 635 Makoto, K., Shibata, H., Kim, Y., Satomura, T., Takagi, K., Nomura, M., Satoh, F., and Koike, T.: Contribution of charcoal to short-term nutrient dynamics after surface fire in the humus layer of a dwarf bamboo-dominated forest, *Biology and Fertility of Soils*, 48, 569–577, <https://doi.org/10.1007/s00374-011-0657-y>, 2012.
- Malhi, Y., Baldocchi, D., and Jarvis, P.: The carbon balance of tropical, temperate and boreal forests, *Plant, Cell & Environment*, 22, 715–740, <https://doi.org/10.1046/j.1365-3040.1999.00453.x>, 1999.
- 640 Marklund, L.: Biomass functions for Norway spruce (*Picea abies* (L.) Karst.) in Sweden [biomass determination, dry weight], Rapport-Sveriges Lantbruksuniversitet, Institutionen foer Skogstaxering (Sweden), 1987.
- Mekonnen, Z. A., Riley, W. J., Randerson, J. T., Grant, R. F., and Rogers, B. M.: Expansion of high-latitude deciduous forests driven by interactions between climate warming and fire, *Nature plants*, 5, 952–958, <https://doi.org/10.1038/s41477-019-0495-8>, 2019.
- Murphy, P. N., Ogilvie, J., Connor, K., and Arp, P. A.: Mapping wetlands: a comparison of two different approaches for New Brunswick, Canada, *Wetlands*, 27, 846–854, [https://doi.org/10.1672/0277-5212\(2007\)27\[846:MWACOT\]2.0.CO;2](https://doi.org/10.1672/0277-5212(2007)27[846:MWACOT]2.0.CO;2), 2007.
- 645 Naturvårdsverket: Markfuktighetsindex producerat som del av Nationella marktäckedata, NMD, <https://metadatakatalogen.naturvardsverket.se/metadatakatalogen/GetMetaDataById?id=cae71f45-b463-447f-804f-2847869b19b0>, 2018.

- Neary, D. G., Klopatek, C. C., DeBano, L. F., and Ffolliott, P. F.: Fire effects on belowground sustainability: a review and synthesis, *Forest ecology and management*, 122, 51–71, [https://doi.org/10.1016/S0378-1127\(99\)00032-8](https://doi.org/10.1016/S0378-1127(99)00032-8), 1999.
- 650 Neff, J., Harden, J., and Gleixner, G.: Fire effects on soil organic matter content, composition, and nutrients in boreal interior Alaska, *Canadian Journal of Forest Research*, 35, 2178–2187, <https://doi.org/10.1139/x05-154>, 2005.
- Palviainen, M., Pumpanen, J., Berninger, F., Ritala, K., Duan, B., Heinonsalo, J., Sun, H., Köster, E., and Köster, K.: Nitrogen balance along a northern boreal forest fire chronosequence, *PloS one*, 12, <https://doi.org/10.1371/journal.pone.0174720>, 2017.
- Preston, C. M. and Schmidt, M. W.: Black (pyrogenic) carbon: a synthesis of current knowledge and uncertainties with special consideration
655 of boreal regions, *Biogeosciences*, 3, 397–420, <https://doi.org/10.5194/bg-3-397-2006>, 2006.
- QGIS Development Team: QGIS Geographic Information System, QGIS Association, <https://www.qgis.org>, 2019.
- Rabin, S. S., Melton, J. R., Lasslop, G., Bachelet, D., Forrest, M., Hantson, S., Kaplan, J. O., Li, F., Mangeon, S., Ward, D. S., Yue, C., Arora, V. K., Hickler, T., Kloster, S., Knorr, W., Nieradzik, L., Spessa, A., Folberth, G. A., Sheehan, T., Voulgarakis, A., Kelley, D. I., Prentice, I. C., Sitch, S., Harrison, S., and Arneth, A.: The Fire Modeling Intercomparison Project (FireMIP), phase 1: experimental
660 and analytical protocols with detailed model descriptions, *Geoscientific Model Development*, 10, 1175–1197, <https://doi.org/10.5194/gmd-10-1175-2017>, 2017.
- Rapalee, G., Trumbore, S. E., Davidson, E. A., Harden, J. W., and Veldhuis, H.: Soil carbon stocks and their rates of accumulation and loss in a boreal forest landscape, *Global Biogeochemical Cycles*, 12, 687–701, <https://doi.org/10.1029/98GB02336>, 1998.
- Rogers, B. M., Soja, A. J., Goulden, M. L., and Randerson, J. T.: Influence of tree species on continental differences in boreal fires and
665 climate feedbacks, *Nature Geoscience*, 8, 228–234, <https://doi.org/10.1038/ngeo2352>, 2015.
- Ruiz, J. A. M., Riaño, D., Arbelo, M., French, N. H., Ustin, S. L., and Whiting, M. L.: Burned area mapping time series in Canada (1984–1999) from NOAA-AVHRR LTDR: A comparison with other remote sensing products and fire perimeters, *Remote Sensing of Environment*, 117, 407–414, <https://doi.org/10.1016/j.rse.2011.10.017>, 2012.
- Santín, C., Doerr, S. H., Preston, C. M., and González-Rodríguez, G.: Pyrogenic organic matter production from wildfires: a missing sink in
670 the global carbon cycle, *Global Change Biology*, 21, 1621–1633, <https://doi.org/10.1111/gcb.12800>, 2015.
- Santín, C., Doerr, S. H., Merino, A., Bryant, R., and Loader, N. J.: Forest floor chemical transformations in a boreal forest fire and their correlations with temperature and heating duration, *Geoderma*, 264, 71–80, <https://doi.org/10.1016/j.geoderma.2015.09.021>, 2016.
- Schmidt, M. W. and Noack, A. G.: Black carbon in soils and sediments: analysis, distribution, implications, and current challenges, *Global
675 biogeochemical cycles*, 14, 777–793, <https://doi.org/10.1029/1999GB001208>, 2000.
- Schultz, M. G., Heil, A., Hoelzemann, J. J., Spessa, A., Thonicke, K., Goldammer, J. G., Held, A. C., Pereira, J. M. C., and van het Bolscher, M.: Global wildland fire emissions from 1960 to 2000, *Global Biogeochemical Cycles*, 22, <https://doi.org/10.1029/2007GB003031>, 2008.
- Schweiger, A. H., Irl, S. D. H., Steinbauer, M. J., Dengler, J., and Beierkuhnlein, C.: Optimizing sampling approaches along ecological gradients, *Methods in Ecology and Evolution*, 7, 463–471, <https://doi.org/10.1111/2041-210X.12495>, 2016.
- 680 Seabold, S. and Perktold, J.: statsmodels: Econometric and statistical modeling with python, in: 9th Python in Science Conference, <http://dx.doi.org/10.25080/Majora-92bf1922-011>, 2010.
- Sidoroff, K., Kuuluvainen, T., Tanskanen, H., and Vanha-Majamaa, I.: Tree mortality after low-intensity prescribed fires in managed *Pinus sylvestris* stands in southern Finland, *Scandinavian Journal of Forest Research*, 22, 2–12, <https://doi.org/10.1080/02827580500365935>, 2007.

- 685 Soja, A. J., Cofer, W. R., Shugart, H. H., Sukhinin, A. I., Stackhouse, P. W., McRae, D. J., and Conard, S. G.: Estimating fire emissions and disparities in boreal Siberia (1998–2002), *Journal of Geophysical Research: Atmospheres*, 109, <https://doi.org/10.1029/2004JD004570>, 2004.
- Stocks, B. J., Mason, J. A., Todd, J. B., Bosch, E. M., Wotton, B. M., Amiro, B. D., Flannigan, M. D., Hirsch, K. G., Logan, K. A., Martell, D. L., and Skinner, W. R.: Large forest fires in Canada, 1959–1997, *Journal of Geophysical Research: Atmospheres*, 107, FFR 5–1–FFR 690 5–12, <https://doi.org/10.1029/2001JD000484>, 2002.
- Tagesson, T., Schurgers, G., Horion, S., Ciais, P., Tian, F., Brandt, M., Ahlström, A., Wigneron, J.-P., Ardö, J., Olin, S., Fan, L., Wu, Z., and Fensholt, R.: Recent divergence in the contributions of tropical and boreal forests to the terrestrial carbon sink, *Nature Ecology and Evolution*, 4, <https://doi.org/10.1038/s41559-019-1090-0>, 2020.
- Valendik, E.: Temporal and spatial distribution of forest fires in Siberia, in: *Fire in Ecosystems of Boreal Eurasia*, pp. 129–138, Springer, 695 https://doi.org/10.1007/978-94-015-8737-2_9, 1996.
- Vallat, R.: Pingouin: statistics in Python, *The Journal of Open Source Software*, 3, 1026, <https://doi.org/10.21105/joss.01026>, 2018.
- van der Werf, G. R., Randerson, J. T., Giglio, L., van Leeuwen, T. T., Chen, Y., Rogers, B. M., Mu, M., van Marle, M. J. E., Morton, D. C., Collatz, G. J., Yokelson, R. J., and Kasibhatla, P. S.: Global fire emissions estimates during 1997–2016, *Earth System Science Data*, 9, 697–720, <https://doi.org/10.5194/essd-9-697-2017>, 2017.
- 700 van Leeuwen, T. T., van der Werf, G. R., Hoffmann, A. A., Detmers, R. G., Rücker, G., French, N. H. F., Archibald, S., Carvalho Jr., J. A., Cook, G. D., de Groot, W. J., Hély, C., Kasischke, E. S., Kloster, S., McCarty, J. L., Pettinari, M. L., Savadogo, P., Alvarado, E. C., Boschetti, L., Manuri, S., Meyer, C. P., Siegert, F., Trollope, L. A., and Trollope, W. S. W.: Biomass burning fuel consumption rates: a field measurement database, *Biogeosciences*, 11, 7305–7329, <https://doi.org/10.5194/bg-11-7305-2014>, 2014.
- Van Wagner, C.: Development and structure of the canadian forest fire weather index system, in: *Can. For. Serv., Forestry Tech. Rep.*, Citeseer, 705 1987.
- Vanhala, P., Karhu, K., Tuomi, M., Björklöf, K., Fritze, H., and Liski, J.: Temperature sensitivity of soil organic matter decomposition in southern and northern areas of the boreal forest zone, *Soil biology and biochemistry*, 40, 1758–1764, <https://doi.org/10.1016/j.soilbio.2008.02.021>, 2008.
- Veraverbeke, S., Rogers, B. M., and Randerson, J. T.: Daily burned area and carbon emissions from boreal fires in Alaska, *Biogeosciences*, 710 12, 3579–3601, <https://doi.org/10.5194/bg-12-3579-2015>, 2015.
- Virtanen, P., Gommers, R., Oliphant, T. E., Haberland, M., Reddy, T., Cournapeau, D., Burovski, E., Peterson, P., Weckesser, W., Bright, J., van der Walt, S. J., Brett, M., Wilson, J., Millman, K. J., Mayorov, N., Nelson, A. R. J., Jones, E., Kern, R., Larson, E., Carey, C. J., Polat, İ., Feng, Y., Moore, E. W., VanderPlas, J., Laxalde, D., Perktold, J., Cimrman, R., Henriksen, I., Quintero, E. A., Harris, C. R., Archibald, A. M., Ribeiro, A. H., Pedregosa, F., van Mulbregt, P., and SciPy 1.0 Contributors: SciPy 1.0: Fundamental Algorithms for Scientific 715 Computing in Python, *Nature Methods*, 17, 261–272, <https://doi.org/10.1038/s41592-019-0686-2>, 2020.
- Walker, X., Rogers, B., Veraverbeke, S., Johnstone, J., Baltzer, J., Barrett, K., Bourgeau-Chavez, L., Day, N., Groot, W., Dieleman, C., Goetz, S., Hoy, E., Jenkins, L., Kane, E., Parisien, M.-A., Potter, S., Schuur, E., Turetsky, M., Whitman, E., and Mack, M.: Fuel availability not fire weather controls boreal wildfire severity and carbon emissions, *Nature Climate Change*, pp. 1–7, <https://doi.org/10.1038/s41558-020-00920-8>, 2020.
- 720 Walker, X. J., Rogers, B. M., Baltzer, J. L., Cumming, S. G., Day, N. J., Goetz, S. J., Johnstone, J. F., Schuur, E. A. G., Turetsky, M. R., and Mack, M. C.: Cross-scale controls on carbon emissions from boreal forest megafires, *Global Change Biology*, 24, 4251–4265, <https://doi.org/10.1111/gcb.14287>, 2018.

- Waskom, M. and the seaborn development team: mwaskom/seaborn, Zenodo, <https://doi.org/10.5281/zenodo.592845>, 2020.
- Wiggins, E. B., Andrews, A., Sweeney, C., Miller, J. B., Miller, C. E., Veraverbeke, S., Commane, R., Wofsy, S., Henderson, J. M., and
725 Randerson, J. T.: Evidence for a larger contribution of smoldering combustion to boreal forest fire emissions from tower observations in
Alaska, *Atmospheric Chemistry and Physics Discussions*, 2020, 1–26, <https://doi.org/10.5194/acp-2019-1067>, 2020.
- Wilcke, R. A. I., Kjellström, E., Lin, C., Matei, D., Moberg, A., and Tyrlis, E.: The extremely warm summer of 2018 in Sweden – set in a
historical context, *Earth System Dynamics*, 11, 1107–1121, <https://doi.org/10.5194/esd-11-1107-2020>, 2020.
- Wooster, M. J. and Zhang, Y. H.: Boreal forest fires burn less intensely in Russia than in North America, *Geophysical Research Letters*, 31,
730 <https://doi.org/10.1029/2004GL020805>, 2004.
- Zackrisson, O., Nilsson, M.-C., and Wardle, D. A.: Key ecological function of charcoal from wildfire in the Boreal forest, *Oikos*, pp. 10–19,
<https://doi.org/10.2307/3545580>, 1996.
- Zoltai, S., Morrissey, L., Livingston, G., and Groot, W. d.: Effects of fires on carbon cycling in North American boreal peatlands, *Environmental Reviews*, 6, 13–24, <https://doi.org/10.1139/a98-002>, 1998.

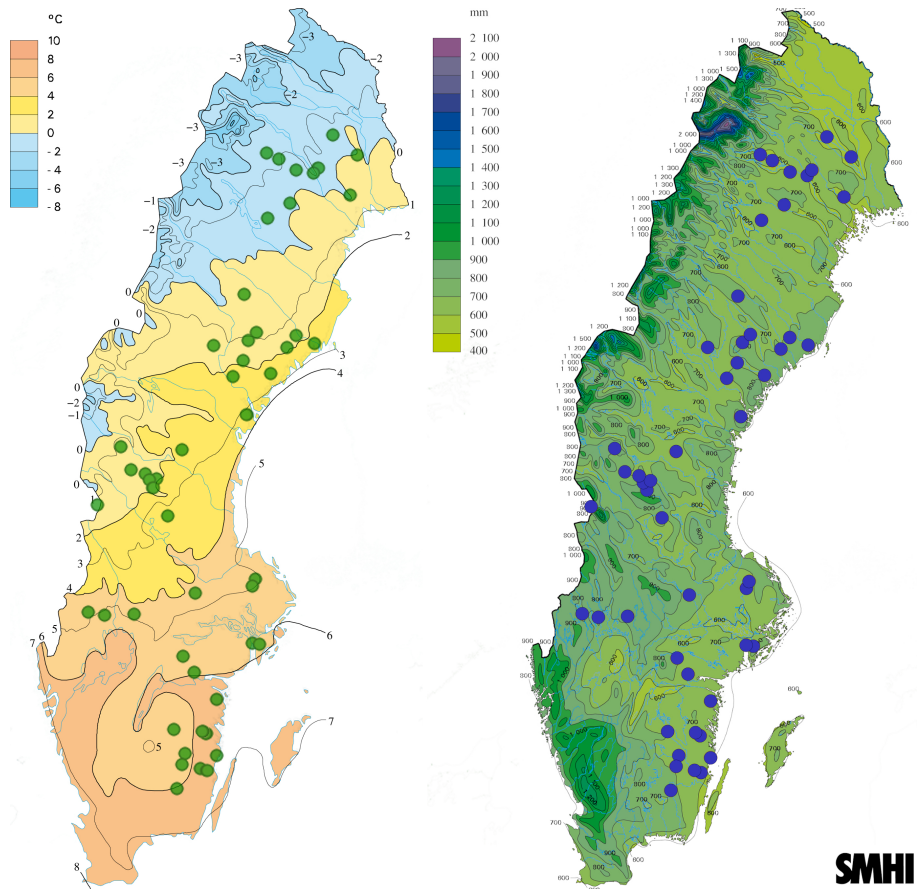


Figure 1. Using climate data averaged over the period 1961-2017 provided by the Swedish Meteorological and Hydrological Institute (SMHI) for plot selection, MAT had a range of 0.43-7.77 °C and MAP of 539-772 mm over an approximately 57-67° latitudinal change. The 50 plot pairs are pictured as points upon MAT and MAP gradients over the last normal period 1961-1990.

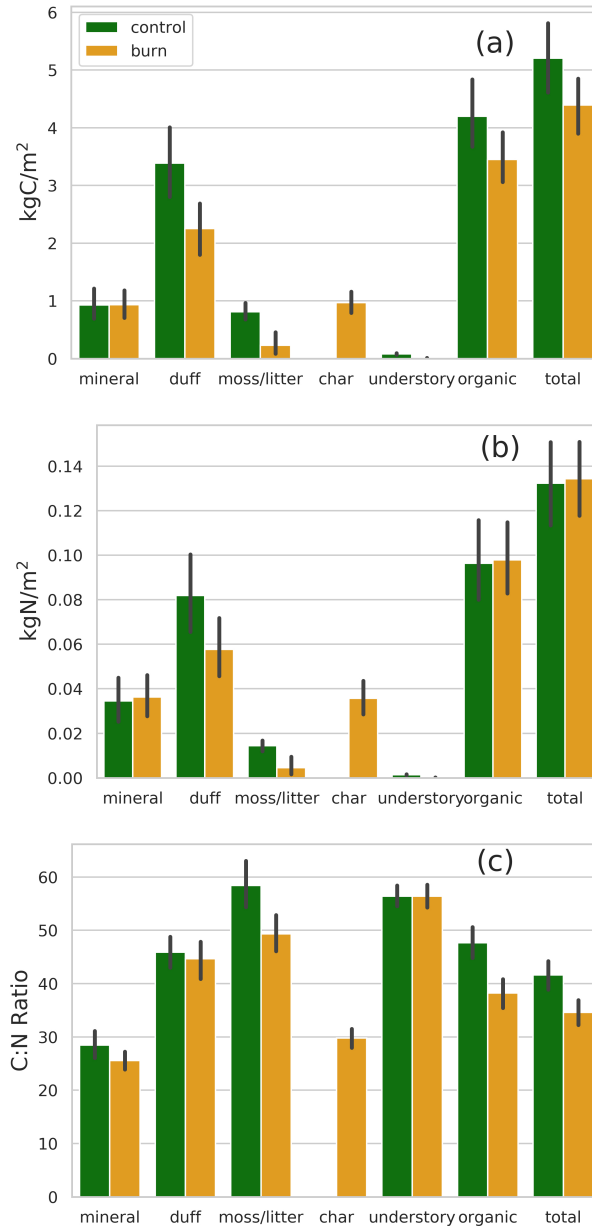


Figure 2. Mean C (a) and N (b) stocks and their ratio (c) between burnt and control plots amongst forest compartments. The organic category is considered the grouping of the duff, moss/litter and char layers while the total category is the grouping of the organic and mineral soil layers along with the understory. Error bars are the bootstrapped 95% confidence interval of the mean.

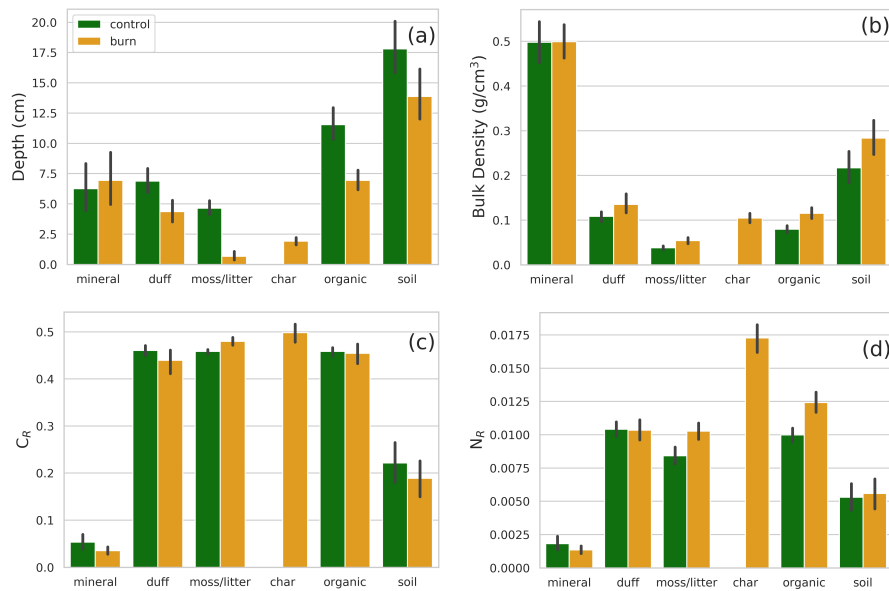


Figure 3. Mean soil compartment depths (a), bulk density (b), C_R (c), and N_R (d) in burnt and control plots. The organic category is considered the grouping of the duff, moss/litter and char layers while the soil category is the grouping of the organic and mineral soil layers. Error bars are the bootstrapped 95% confidence interval of the mean.

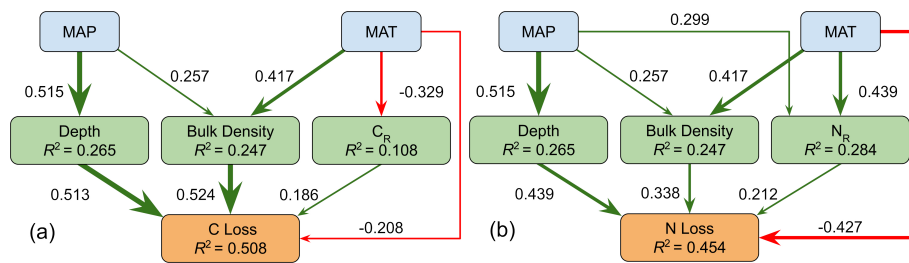


Figure 4. Diagram of proposed pathways for the effects of MAP and MAT on C (a) and N (b) loss. Non climate variables regard the organic layer. Each variable node is labeled with the R^2 from simple or multiple regression using explanatory variables represented by all incoming arrows. Arrows are labeled by and sized in proportion to the magnitude of their standardized regression coefficients. Green arrows represent positive relationships while red represent negative relationships. Omitted for simplicity are direct correlations between bulk density and C_R ($p = 0.010$, $r = 0.356$) and depth and N_R ($p = 0.010$, $r = -0.363$)

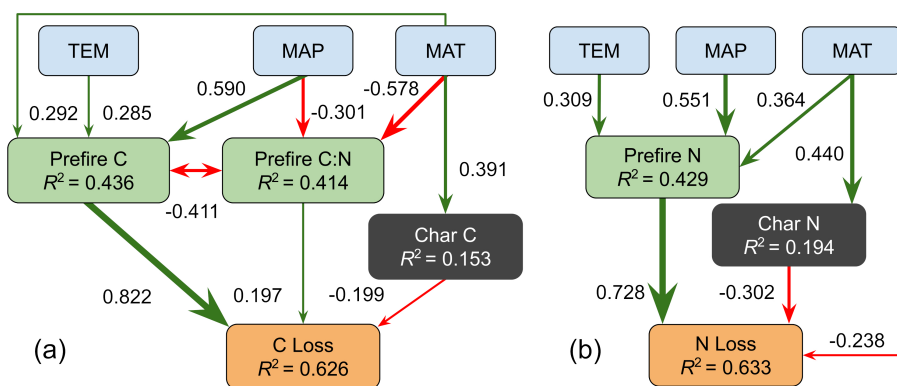


Figure 5. Path diagrams for C (a) and N (b) loss including char and C:N variables. Prefire C, N, and C:N as well as losses of C and N are regarding the organic layer. Each variable node is labeled with the R^2 from simple or multiple regression using explanatory variables represented by all incoming arrows. Arrows are labeled by and sized in proportion to the magnitude of their standardized regression coefficients. Green arrows represent positive relationships while red represent negative relationships.

Table 1. Mean values of distributions ($n = 50$) formed by subtracting control plot variables from their paired burnt plot. In parentheses are first the 95% confidence interval of the distribution and then the percentage change calculated from the overall means of control and burnt plots. Statistically significant fire-induced changes are in bold.

	C ($kg\ m^{-2}$)	N ($kg\ m^{-2}$)	C:N
Total	-0.815 (0.652, -15.6)	0.00208 (0.0184, 1.6)	-7.01 (2.58, -16.8)
Understory	-0.0717 (0.0126, -90.6)	-0.00127 (0.000224, -90.6)	– (–, –)
Soil	-0.744 (0.651, -14.5)	0.00336 (0.0184, 2.6)	-6.88 (2.61, -16.6)
Organic	-0.747 (0.633, -17.8)	0.00157 (0.0187, 1.6)	-9.46 (2.97, -19.8)
Char	0.971 (0.182, –)	0.0357 (0.00799, –)	– (–, –)
Moss/Litter	-0.584 (0.258, -72.0)	-0.00985 (0.00490, -68.2)	-9.09 (4.01, -15.6)
Duff	-1.13 (0.581, -33.5)	-0.0242 (0.0173, -29.6)	-1.24 (3.32, -2.7)
Mineral	0.00333 (0.248, 0.4)	0.00179 (0.00834, 5.2)	-3.11 (2.46, -10.2)

Table 2. Mean values of distributions ($n = 50$) formed by subtracting control plot variables from their paired burnt plot. In parentheses are first the 95% confidence interval of the distribution and then the percentage change calculated from the overall means of control and burnt plots. Statistically significant fire-induced changes are in bold.

	Depth (cm)	Bulk Density ($g\ cm^{-3}$)	C_r	N_r
Soil	-3.92 (1.47, -22.0)	0.0665 (0.0305, 30.7)	-0.0326 (0.0395, -14.7)	0.000286 (0.00104, 5.4)
Organic	-4.60 (1.19, -39.9)	0.0358 (0.0110, 45.0)	-0.00402 (0.0193, -0.9)	0.00243 (0.000801, 24.3)
Char	1.91 (0.292, -)	- (-, -)	- (-, -)	- (-, -)
Moss/Litter	-3.98 (0.762, -85.6)	0.0162 (0.00568, 42.8)	0.0215 (0.00828, 4.7)	0.00185 (0.000727, 21.9)
Duff	-2.53 (1.04, -36.8)	0.0270 (0.0190, 24.9)	-0.0212 (0.0239, -4.6)	-0.0000714 (0.000714, -0.7)
Mineral	0.684 (1.32, 10.9)	0.00565 (0.0352, 0.283)	-0.0199 (0.0127, -34.2)	-0.000505 (0.000369, -25.8)